An Experimental and Theoretical Investigation of the Photophysics of 1-Hydroxy-2-naphthoic Acid

H. Mishra,[†,‡] S. Maheshwary,[§] H. B. Tripathi,*[,†,∥] and N. Sathyamurthy*[,§,⊥]

Photophysics Laboratory, Department of Physics, Kumaun University, Nainital 263 001, India, and Department of Chemistry, Indian Institute of Technology Kanpur, Kanpur 208016, India

Received: August 28, 2004; In Final Form: December 17, 2004

Photophysical and photochemical properties of 1-hydroxy-2-naphthoic acid (1,2-HNA) have been investigated experimentally by steady state and time domain fluorescence measurements and theoretically by Hartree−Fock (HF), configuration interaction at the single excitation (CIS) level, density functional theoretic (DFT), and semiempirical (AM1) methods. 1,2-HNA exhibits normal fluorescence that depends on its concentration, nature of the solvent, pH, temperature, and wavelength of excitation. It seems to form different emitting species in different media, akin to 3-hydroxy-2-naphthoic acid (3,2-HNA). The large Stokes shifted emission observed at pH 13 is attributed to species undergoing excited-state intramolecular proton transfer. Nonradiative transition seems to increase on protonation and decrease on deprotonation. AM1(PECI=8) calculations predict the absorption maximum (λ_{max} = 335.9 nm) in reasonable agreement with experiment (λ_{max} = 352 nm) for the neutral 1,2-HNA. They also predict a red shift in absorption on protonation and a blue shift on deprotonation as observed experimentally. CIS calculations tend to overestimate the energy gap and hence underestimate the absorption maxima between the ground and the excited electronic states of 1,2-HNA and its protonated and deprotonated forms. However, they do predict correctly that the excited state intramolecular proton transfer is likely to occur in the deprotonated form of 1,2-HNA and not in the neutral and the protonated forms. A single minimum is found in the potential energy profile for the ground state as well as the first excited state of 1,2-HNA and its protonated species. In contrast, a double minimum with a nominal barrier in between is predicted for the ground state and also the first three excited states of the deprotonated species. The keto form of the deprotonated species is found to be slightly less stable than the enol form in all the states investigated.

1. Introduction

Ground- and excited-state intramolecular proton transfers in salicylic acid (SA) and related systems have been the subject of experimental and theoretical investigations for the last several decades (see refs 1−4 and references therein). When an −OH group and a −COOH group are present in a naphthalene system, several possible combinations arise, but only three of them are salicylic acid-like in that the −OH and the −COOH groups are ortho to each other and form intramolecular hydrogen bonding (IMHB) as illustrated in Figure 1.

It is well-known that depending on the position of the substituents, the electronic spectrum of a substrate gets modified. For 1(α)-substituted naphthalene, for example, the L_a band is lower in energy than the L_b band, but for 2(β)-substituted naphthalene, the L_b band is lower than the L_a band.[5,6] Here the L_a and L_b refer to polarization of the excited state along the axis through the atoms and the axis through the bonds, respectively.[6] It is also known that the lowest energy transition in the case of molecules having cross-linking with the conjugated chain is L_b. Catalán et al.[7] have shown that for methylated 3-hydroxy-2-naphthoic acid (32MHN), the lowest excited state is L_a and for methyl 1-hydroxy-2-naphthoate (12MHN) and methyl 2-hydroxy-1-naphthoate (21MHN), it is L_b. In contrast, it is found that for 1,2-HNA and 3,2-HNA, L_b is the lowest excited fluorescence state, and for 2,1-HNA L_a is the lowest.[5] In 1,2-HNA, the hydroxy group is substituted at the α-position and the carboxylic acid group at the β-position in the naphthalene ring. Thus there is a competition between L_b and L_a bands for lowering in energy in 1,2-HNA and 2,1-HNA, while in 3,2-HNA only the L_b state is lower (both −OH and −COOH groups are in the β-position). Thus L_a and L_b bands play an important role in influencing the photophysics of 1,2-HNA.

It is reported that excited-state intramolecular proton transfer (ESIPT) takes place in 3,2-HNA and not in 1,2-HNA or 2,1-HNA.[8−11] These molecules are of interest in understanding the role of IMHB in ESIPT. *o*-Hydroxynaphthoic acids are of considerable interest as chelating agents, fluorescent indicators, and in the manufacture of dyestuffs.[5] While 3,2-HNA chelates readily, 1,2-HNA and 2,1-HNA are slow in chelation. Kovi and Schulman[10] have identified several species of 3,2-HNA, 2,1-HNA, and 1,2-HNA under different pH conditions through absorption and fluorescence measurements. They also reported that neutral 1,2-HNA and 2,1-HNA undergo biprotonic phototautomerization to their respective zwitterions, while a similar process is not observed in 3,2-HNA. Further they have reported that ESIPT occurs in the 3,2-HNA anion and not in 1,2-HNA and 2,1-HNA in the pH range 6 to 10. On comparing SA and

[†] Kumaun University.
[‡] E-mail: hirdyesh@yahoo.com. Phone: +91-5942-237450. Fax: + 91-5942-235576.
[§] Indian Institute of Technology Kanpur.
[∥] E-mail: herabtripathi@yahoo.com. Phone: +91-5942-236003. Fax: + 91-5942-235576.
[⊥] E-mail: nsath@iitk.ac.in. Phone: +91-512-2597390. Fax: + 91-512-2597390.

10.1021/jp0461091 CCC: $30.25
Published on Web 02/25/2005

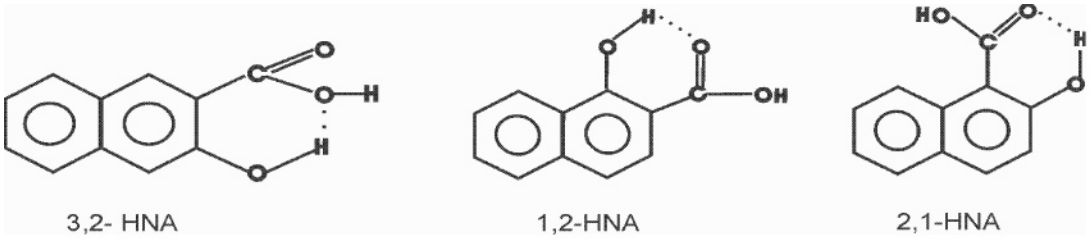

Figure 1. Three different positional isomers of hydroxynaphthoic acid exhibiting intramolecular hydrogen bonding.

TABLE 1: Spectral Properties of 1,2-HNA in Various Media

medium	concn (M)	λ_{abs}^{max} (nm)	λ_{em}^{max} (nm)	Stokes shift (cm^{-1})	lifetime τ (ns)	emitting species
EtOH	10^{-3}	346.0	415.0	4805	1.8, 4.3	neutral, monoanion
EtOH +H^+ (1%)	10^{-3}	352.0	418.0	4485	1.85	neutral
EtOH +OH^- (1%)	10^{-3}	340.0	413.0	4856	1.78, 4.5	neutral, monoanion
conc H_2SO_4	10^{-4}	380.0	452.0	4191	0.85	monocation
6 N KOH	10^{-4}	339.0	463.0	7900	5.6	monoanion
water	10^{-4}	340.0	416.0	5460	1.78, 4.5	neutral, monoanion
cyclohexane	10^{-5}	354.8	398.0	3122	2.43	neutral
cyclohexane + ether	10^{-4}	354.0	398.5	3122	2.45, 5.3	neutral, monoanion
paraffin liquid	Solid	390.0	451.0	3468		dimer
ether	10^{-4}	350.0	390.0	2930		neutral
ether + TEA	10^{-4}	350.0	390.0	2930		neutral, monoanion
dioxane	10^{-4}	354.0	395.0	2932	2.31, 5.57	neutral, monoanion
acetonitrile	10^{-4}	370.0	418.0	3103		neutral, monoanion

3,2-HNA they found[11] that the paths of ionization in the ground and excited states are different.

The photophysics of methyl 3-hydroxy-2-naphthoate and phenyl 1-hydroxy-2-naphthoate was investigated by Woolfe and Thistlethwaite.[12] They found that the former gave rise to large Stokes shifted emission, while the latter exhibited only normal emission. This difference has been attributed to the difference in the acid−base properties of the two species. Law and Shoham[13] also reported on the photophysics of 32MHN in nonpolar and polar solvents and found ESIPT to be solvent and temperature dependent. The stability of intra- and intermolecular hydrogen bonds in SA, HNA, and 2,6-dihydroxybenzoic acid (DHBA) has been studied by Golubev et al.[14] from their NMR and IR spectra.

Recently Catalán et al.[7] have studied the ESIPT in the esters of *o*-hydroxynaphthoic acids and compared the results with those for methyl salicylate and found that the photostability of these compounds is independent of the photophysics of their proton-transfer tautomers but depends on the nonradiative dynamics of their respective normal tautomers. By a comparative study of 12MHN, 21MHN, and 32MHN, they found that the photophysics of these compounds was influenced by the position of the IMHB in these molecules. Based on molecular orbital calculations, they have suggested that the first and second excited states have $\pi\pi^*$ character. Substitution of a phenyl ring in the α-position in naphthoic acid causes level inversion, while in the β-position no such level inversion takes place.[15] Recently Banerjee et al.[16] have studied 3,7-dihydroxy-2-naphthoic acid in protic and aprotic solvents and found evidence for the existence of both the monomer and the dimer in very dilute solutions. They also proposed that addition of a base promotes proton transfer in polar protic solvents only.

In the present work systematic spectral, kinetic, and electronic structure studies of 1,2-HNA have been carried out under different conditions of solvent and pH and a comparison is made with the results for 3,2-HNA. To the best of our knowledge, no other time domain study and electronic structure calculation have been reported for 1,2-HNA till this date.

2. Methodology

1,2-HNA obtained from Aldrich was purified by dissolving it in ethanol and precipitating it out by adding deionized water and then re-crystallizing from ethanol. All the solvents used were of spectroscopic grade (Aldrich) and were used without further purification.

Absorption spectra of 1,2-HNA were taken with the help of a JASCO V-550 spectrophotometer and corrected fluorescence and excitation spectra were recorded on a JASCO FP-777[17] spectrofluorometer. Decay time measurements were carried out using the single photon counting technique in an Edinburgh spectrofluorometer EI-199[18] and analyzed with the help of the proprietary software FLA-900. It is worth mentioning that the excitation source was a thyratron gated nanosecond flash lamp with hydrogen as the filler gas. Lamp profiles were measured at the excitation wavelength with a Ludox scatterer. The pulse width was about 1 ns with a repetition rate of 20 kHz. The intensity decay curves so obtained were fitted to a sum of exponential terms:

$$I(\tau,t) = \alpha_1 \exp(-t/\tau_1) + \alpha_2 \exp(-t/\tau_2) \qquad (1)$$

where τ_1 and τ_2 are the lifetime components and α_1 and α_2 are the corresponding amplitudes. Weighted residuals and χ^2 values were used to judge the goodness of the fit. Low-temperature measurements were carried out in liquid nitrogen by keeping the sample in a sample holder in a quartz dewar. The relative quantum yield of fluorescence (f_s) of the sample was calculated by using the relation $\phi_s = (\phi_r A_r F_s n_s^2)/(A_s F_r n_r^2)$, where the indices s and r refer to the sample and the reference, respectively. Quinine sulfate dication was used as the reference, with $\phi_r = 0.54$. *A* represents absorbance at 300 nm, *F* is the fluorescence area, and *n* is the refractive index.

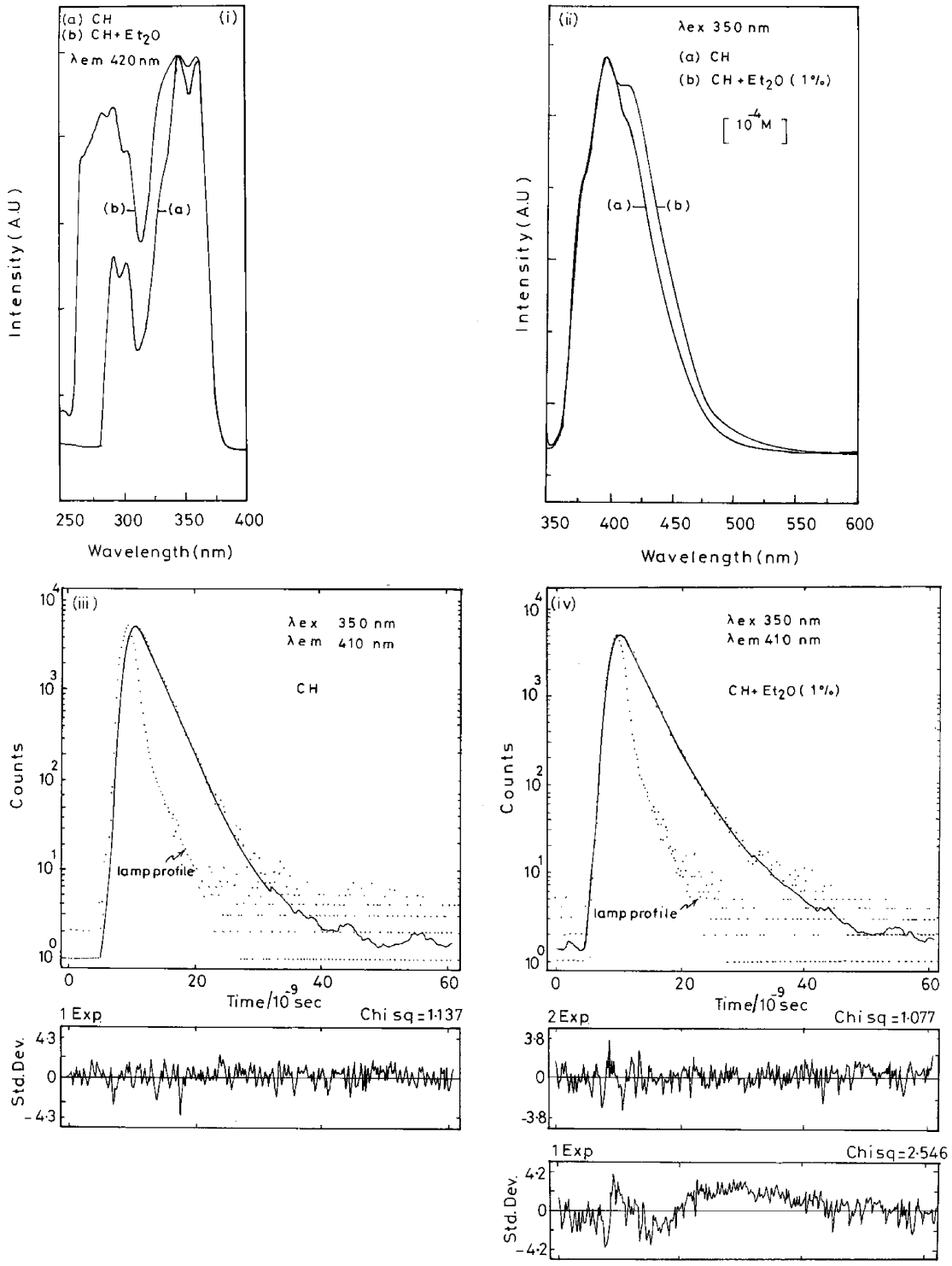

Figure 2. (i) Excitation and (ii) normalized emission spectrum of 10^{-4} M 1,2-HNA in (a) cyclohexane and (b) cyclohexane + ether (1%) mixture. The fluorescence decay curves of 1,2-HNA (10^{-4} M) in cyclohexane and in cyclohexane + ether (1%) mixture are reproduced in parts iii and iv, respectively. The respective distribution of residuals and χ^2 values for single and biexponential fits are given below the fitted decay curves.

Ab initio and density functional theoretic (DFT) calculations were carried out with the GAUSSIAN 94 suite of programs.[19] Hartree−Fock (HF) calculations with different basis sets suggested 6-31G** to be the optimal basis set in terms of the price−performance ratio for carrying out elaborate potential-energy curve scans and determining the strength of intramolecular hydrogen bonding and relative stabilities of species. Semiempirical (AM1) calculations were carried out with MOPAC-6, particularly for determining the absorption maximum (λ_{abs}^{max}) for the different species.

3. Results and Discussion

3.1. Experimental. The various steady state and time domain fluorescence data obtained for 1,2-HNA in different solvents are given in Table 1.

3.1.1. In Nonpolar Solvents. The excitation and emission spectra of 1,2-HNA in cyclohexane at 10^{-4} M concentration are shown in Figure 2, parts i and ii, respectively. The excitation spectrum shows absorption maxima around 354 nm (L_b) and around 298 nm (L_a) and the emission occurs at 398 nm, with a

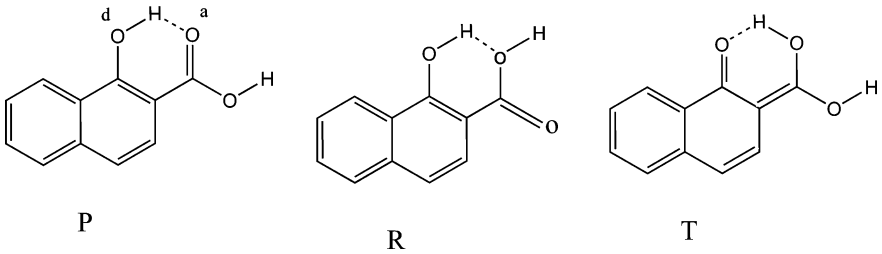

Figure 3. P, R, and T forms of 1,2 HNA; d and a represent the donor and acceptor oxygen atoms in the P form.

TABLE 2: Comparison of Relative Energies and Strengths of Intramolecular Hydrogen Bonds (IMHB) in Different Conformers of 1,2-HNA and in Protonated and Deprotonated Forms in Their Ground Electronic States (in kcal/mol)

		1,2-HNA			3,2-HNA		
	species	HF/6-31G**	DFT B3LYP/6-31G**//AM1	AM1 (PECI=8)	HF/6-31G**	DFT B3LYP/6-31G**//AM1	AM1 (PECI=8)
relative stability	P	0.0	0.0	0.0	0.0	0.0	0.0
	R	4.0	3.8	1.6	3.5	3.4	1.6
	T	18.5	16.1	13.3	30.3	27.6	26.5
IMHB	P	14.9	14.0	6.5	9.7	10.2	4.6
	R	10	10.5	4.6	5.4	7.3	2.8
	T	25.8	22.6	14.9	30.0	25.4	16.0
	P($+H^+$)	1.4			3.6		
	P($-H^+$)	30.3	28.4	16.9	25.4	25.3	15.1

Stokes shift of 3120 cm^{-1}. The intensity of the L_a band is less than that of the L_b band. The excitation and emission spectra are independent of the wavelength of emission and excitation, respectively. The decay of the emission is exponential, with a decay time (τ) of 2.45 ns as shown in Figure 2iii. The goodness of the fit is reflected in the plot of the residual and χ^2 values are included in the figure.

On increasing the concentration, a red shift in absorption and a slight blue shift in emission are observed. In liquid paraffin and in solid state, 1,2-HNA shows an absorption maximum at 390 nm and the corresponding emission at 451 nm, with a Stokes shift of 3468 cm^{-1}. This emission band could be due to the dimer of 1,2-HNA. On lowering the temperature (up to 80 K) the emission spectrum shifts toward longer wavelengths, showing increased stabilization of the dimer.

On adding diethyl ether (1%), enhancement in the excitation spectrum with a slight blue shift in absorption and a slight red shift in emission is observed (Figure 2i,ii). This must be due to the increase in monomer content arising from the breakup of the dimer due to interaction with the ether. In the presence of diethyl ether, fluorescence decay becomes biexponential, with decay times of 2.4 (95%) and 5.3 ns (5%) [Figure 2iv]. The distribution of the residuals and χ^2 values for a single exponential fit and a double exponential fit are given below the fitted curve. The longer decay time is presumably due to the monoanion that becomes noticeable in the presence of the ether, as was found for 3,2-HNA.[3,25]

No ESIPT band is observed in emission although the presence of IMHB [C═O···H−O] has been confirmed by IR studies.[14] It is tempting to conclude from the absence of the ESIPT band that the R form is dominant (see Figure 3 for the definition of P, R, and T forms). However, ab initio calculations (see below) show that this is unlikely because the R form is less stable than the P form by ∼4 kcal/mol (see Table 2). In addition, it should be pointed out that the barrier for the transformation of the P form to the T form in the excited state is large enough to prevent the ESIPT.

3.1.2. In Polar Solvents. Absorption, excitation, and emission spectra of the 10^{-4} M solution of 1,2-HNA in ethanol under different pH conditions are shown in Figure 4 (parts i, ii, and iii). Four absorption maxima are observed under neutral condition. The L_b band occurs at ∼346 nm and the L_a band at ∼300 nm. The optical density of the L_b band is higher than that of the L_a band. In the excitation spectrum, on monitoring the emission at 425 nm [Figure 4ii (a)], only three bands were observed at the same wavelength as in the absorption spectrum. The intensity of the 250 nm band is decreased and the band at 225 nm disappears due to reduction in the transmission by the fluorescence sample cuvette. The emission spectrum [Figure 4iii (a)] shows a maximum at ∼415 nm, with a Stokes shift of 4805 cm^{-1}. The emission band is found to be independent of the wavelength of excitation and concentration.

On adding 1% of a 6 N KOH solution to the ethanolic solution of 1,2-HNA, the first absorption band (L_b) undergoes a slight blue shift by 6 nm to ∼340 nm, while the second band (L_a) shifts toward red by 15 nm (λ_{max} ∼ 315 nm), There is also a concomitant decrease in optical density and an increase in Stokes shift (4856 cm^{-1}) as well as the full width at half-maximum (fwhm) of the emission band, as shown in Figure 4iii (b). Similar results are observed in the excitation spectrum as shown in Figure 4ii (b).

On adding 1% of a concentrated H_2SO_4 solution, the absorption spectrum becomes more structured, with an increase in the optical density and a slight red shift of 6 nm in the L_b band (λ_{max} ∼ 352 nm) and a blue shift of 20 nm in the L_a band (λ_{max} ∼ 280 nm) as illustrated in Figure 4i (c). Similar results are observed in the excitation spectrum plotted in Figure 4ii (c). Emission is observed at 418 nm, with a decreased fwhm and a decreased Stokes shift (4485 cm^{-1}) relative to the neutral solution [Figure 4iii (c)].

The fluorescence decay in pure ethanol is biexponential in nature, with decay times of 1.8 (85%) and 4.3 ns (15%) as shown in Figure 4iv (a). In the presence of 1% of 6 N KOH solution, the amplitude corresponding to the longer decay time increases with decay times of 1.7 (40%) and 4.5 ns (60%) [Figure 4iv (b)]. However, in the presence of the acid (1%), a monoexponential decay with a decay time of 1.85 ns is observed [Figure 4iv (c)].

Although the ionization constant of 1,2-HNA is low, ionization does occur at low concentrations in ethanolic solutions, as was observed for SA[1] and 3,2-HNA[3]. This indicates that the intramolecular hydrogen bonding is very strong (see below) and

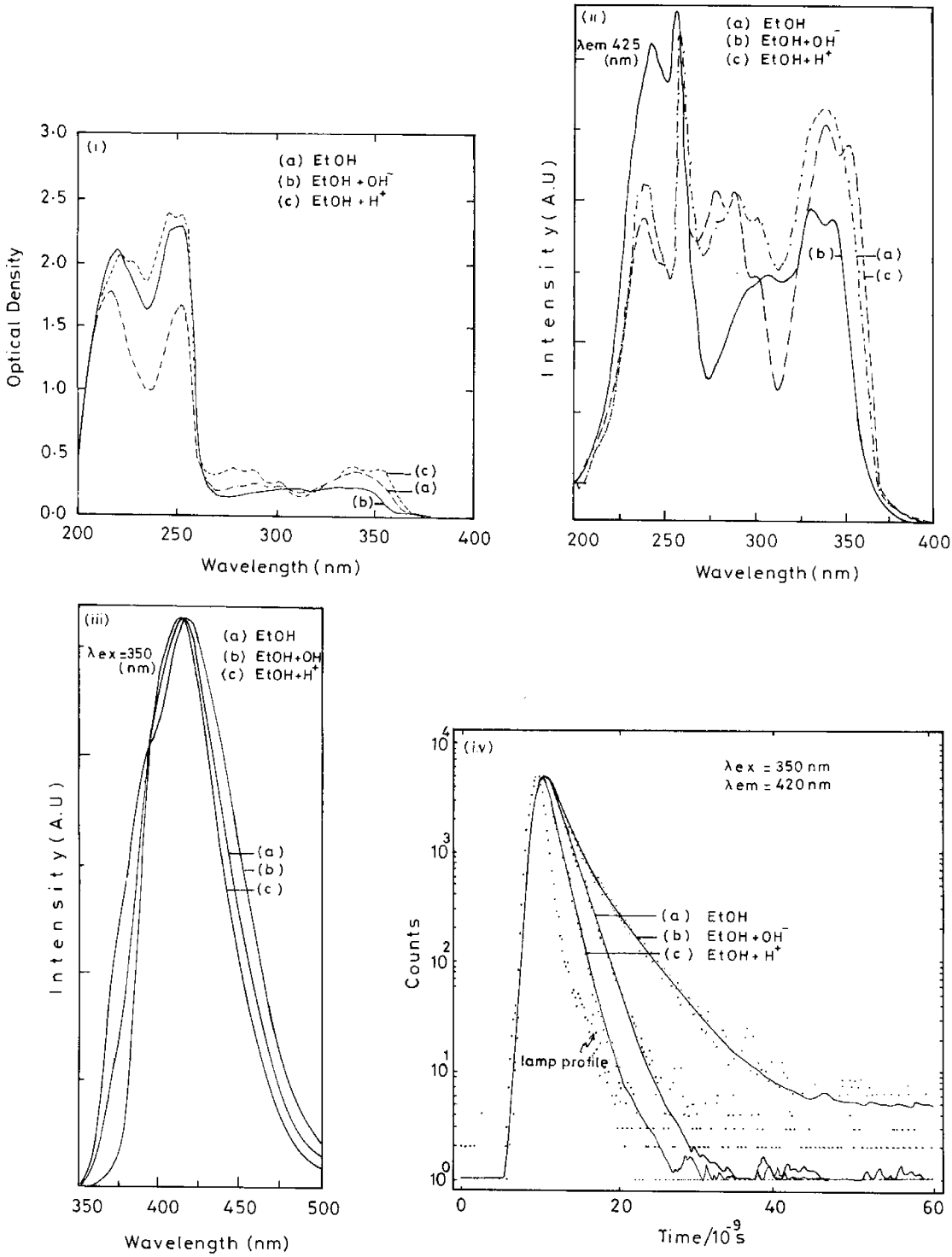

Figure 4. (i) Absorption, (ii) excitation, and (iii) normalized emission spectrum and (iv) fluorescence decay curve for 1,2-HNA (10^{-4}M) in (a) EtOH, (b) EtOH + OH^-, and (c) EtOH + H^+ solutions.

unlike 3,2-HNA no large change in excited-state pK_a takes place.[3] On adding H^+, the protonated species becomes dominant in which nonradiative transition is more and the strength of IMHB decreases. On addition of KOH to a solution of 1,2-HNA in ethanol, 1,2-HNA loses the carboxylic proton to form the monoanion in which nonradiative transition decreases and there is an increase in IMHB strength. To compare this tendency of losing or gaining a proton, we have studied the photoinduced spectral characteristics of 1,2-HNA under high and low pH conditions. The different species originating from 1,2-HNA and their characteristics are summarized in Scheme 1.

3.1.3. Effect of pH. At pH ≫1, absorption maxima for 1,2-HNA (10^{-4} M) are observed (not shown) for the L_b band at 380 nm and the L_a band at 275 nm. The emission maximum occurs at 452 nm with very low fluorescence intensity. It exhibits a Stokes shift of 4190 cm^{-1} and a decay time of 0.85 ns. This emission must be due to the protonated species. In concentrated KOH solution (pH 13), the absorption band has a maximum at 339 nm and the L_b band has merged into the L_a band and the emission peaks at 463 nm, with a Stokes shift of 7900 cm^{-1}. The fluorescence quantum yield is 0.04 and the decay time is 5.6 ns. The large Stokes shifted band is due to ESIPT in the

SCHEME 1

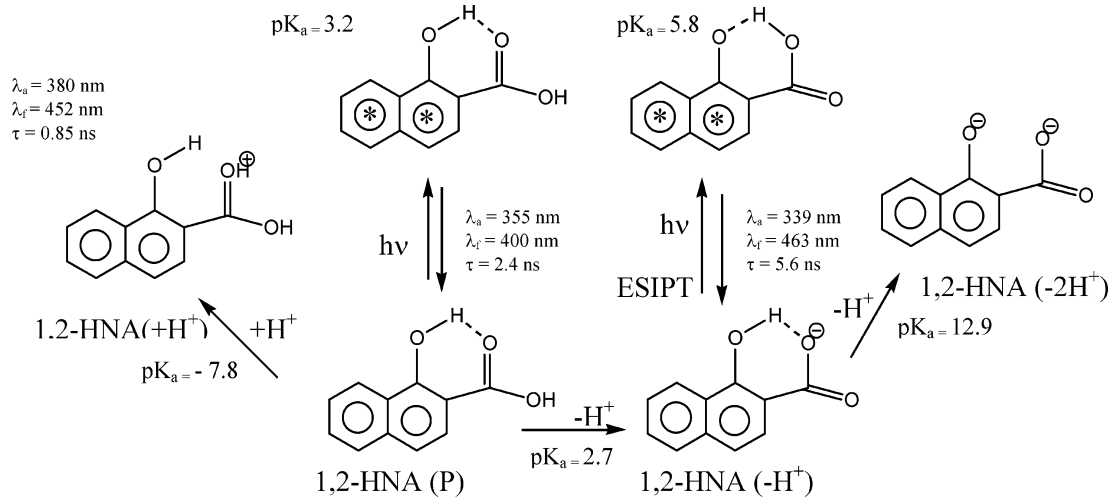

TABLE 3: Spectral Data for 1,2-HNA and Its Protonated and Deprotonated Forms, As Obtained from Theory and Experiment

	experimental		CIS/6-31G**		AM1(PECI=8)	
emitting species	absorption λ_{max} (nm)	Stokes shift (cm^{-1})	absorption λ_{max} (nm)	Stokes shift (cm^{-1})	absorption λ_{max} (nm)	Stokes shift (cm^{-1})
P	352	4485	277.5	2902	335.9	4443
+H$^+$	380	4191	342.2	2298	438.2	6089
-H$^+$	339	7900	286.3	590	311.8	5807

monoanion. Unlike in 3,2-HNA[3], a new absorption band at 460 nm is observed after some time and no emission is observed corresponding to this absorption band. This indicates the stabilization of the keto form of the monoanion due to ground-state intramolecular proton transfer (GSIPT). On further increasing the pH (>13), the absorption band is blue shifted with a Stokes shift of 4550 cm^{-1}. It is expected that like 3,2-HNA[3], 1,2-HNA also exists in a doubly deprotonated form under these conditions and only normal fluorescence is observed. In water (pH ≈7) 1,2-HNA shows a Stokes shift of 5460 cm^{-1}, which is between the high pH and low pH results. In polar solvents, the lowest fluorescence state is L_b. On protonation of the carboxylic acid group, the L_b state becomes lower in energy (red shifted), and on deprotonation the L_b state is shifted to higher energy (blue shifted) and the L_a state becomes lower in energy. Details regarding the photophysics of 1,2-HNA monoanion will be published subsequently.

3.1.4. In Hydrogen Bonding Solvents. In aprotic solvents such as dioxane and ether, 1,2-HNA shows a structured absorption maximum at 350 nm and a corresponding emission at 390 nm with a Stokes shift of 2930 cm^{-1}. This indicates that in hydrogen bonding solvents 1,2-HNA becomes more rigid by forming an intermolecular hydrogen bonding complex. On addition of triethylamine (TEA) no ESIPT band is observed, except for a slight change in the emission spectrum. The decay curve fits to a double exponential function with decay times of 2.3 (88%) and 5.6 ns (12%) corresponding to the neutral and anionic species, respectively.

3.2. Theoretical. *3.2.1. Geometries and Energies.* Ab initio calculations at the HF/6-31G** level predict the P form of 1,2-HNA to be more stable than the R and T by 4.0 and 18.5 kcal/mol, respectively. Here it must be mentioned specifically that the geometry of the P form of 1,2-HNA was optimized first. Then the geometry of the T form was optimized, keeping the O_a-H distance (r_{O_a-H}) the same as the O_d-H distance (r_{O_d-H}) in the optimized geometry of the P form. Otherwise, optimization would lead to the P form! Here O_d and O_a refer to the donor and acceptor oxygen atoms, respectively, in the P form. The geometry of the R form was optimized independently. The transformation from P to R involves the rotation of the carboxylic group with a barrier of 16.1 kcal/mol. The strength of the intramolecular hydrogen bond in P is estimated to be 14.9 kcal/mol and that for the R form is only 10 kcal/mol. Such an estimate was obtained by rotating the phenolic OH group out of the hydrogen bonded configuration and computing the energy difference between the closed and the open forms. AM1 calculations yielded qualitatively similar results as can be seen from Table 2. DFT calculations using AM1 optimized geometries also yielded comparable results as shown in Table 2.

Our earlier experience had shown that AM1 calculations including electron pair excitations at the PECI = 8 level predict the absorption maxima (λ_{max}) in reasonable agreement with experiment for salicylic acid and related systems.[2,3] The AM1-(PECI=8) calculations predict λ_{max} = 335.9 nm, in accord with experiment (λ_{max} = 352 nm) for 1,2-HNA. They also predict qualitatively correctly a red shift on protonation and a blue shift on deprotonation as observed experimentally (see Table 3).

AM1 calculations are not known to be reliable when it comes to predicting potential energy (PE) profiles for intramolecular proton transfer. Hence those results are not reported here.[24]

The transformation from P to T in the ground electronic state can be thought of as arising from a proton transfer from O_d to O_a, with concomitant redistribution of electron density in and around the six-membered hydrogen bonded ring (see Figure 3). Alternatively, one could view this as a hydrogen atom transfer. In either case, one needs to identify the "reaction coordinate" and investigate the potential energy change along the reaction coordinate. Unfortunately, there does not seem to be any simple reaction coordinate definable for the system. It is tempting to consider the stretching of the O_d-H bond distance and the contracting of the $H\cdot\cdot O_a$ distance as constituting the reaction coordinate. Some authors have considered the $O_d\cdot\cdot\cdot O_a$ distance as fixed and varied the O_d-H distance. This may not be desirable, as it puts avoidable constraints on the system. Therefore, we have chosen to vary r_{O_d-H} and optimize the rest of the structural parameters for each choice of r_{O_d-H}. This is

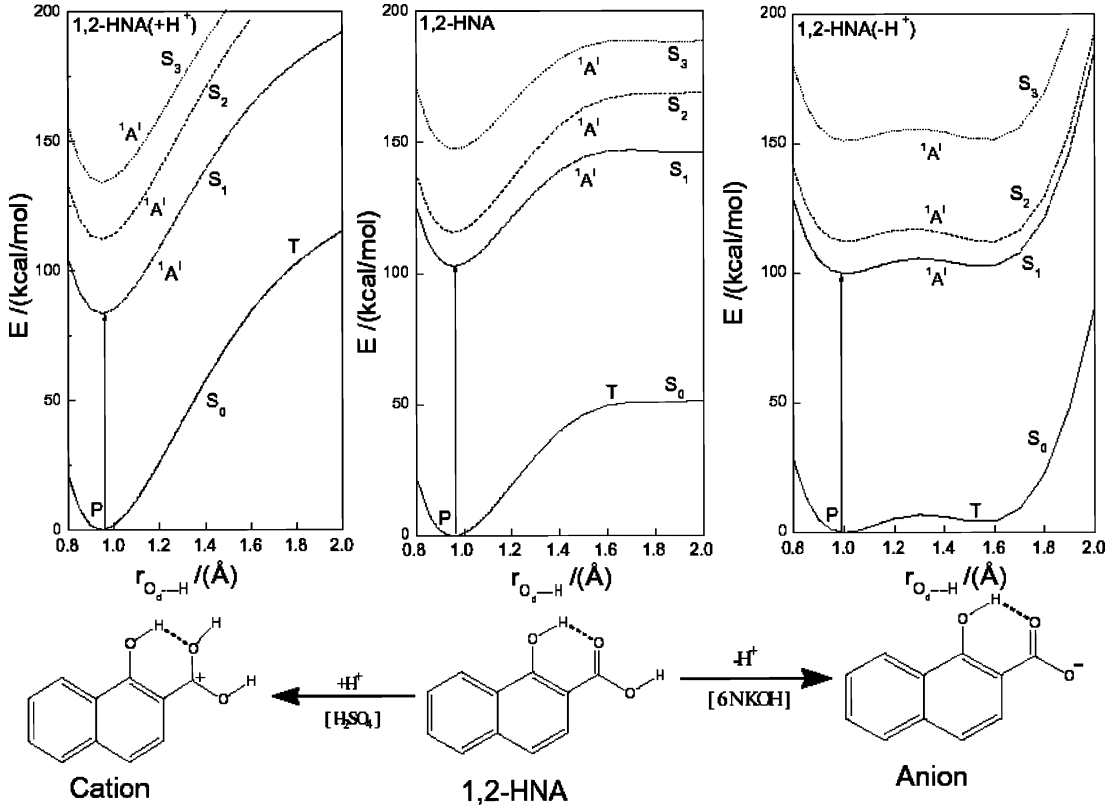

Figure 5. Potential energy profile for intramolecular proton transfer in the ground and excited states of (i) 1,2-HNA and its (ii) protonated and (iii) deprotonated forms, as obtained from CIS/6-31G** calculations.

sometimes referred to as the "distinguished coordinate" approach in the literature.[20] The resulting PE profiles for proton transfer from the P form to the T form of 1,2-HNA in its ground and the first three excited electronic states, as obtained from CIS calculations, are plotted as a function of r_{O_d-H} in Figure 5i. Here it must be mentioned that the CIS optimized geometry was used for the ground electronic state of the P form and r_{O_d-H} was varied as described above. The excited-state PE curves were generated by adding the vertical excitation energies to the ground-state energy for each geometry. The absorption maximum for the P form was predicted to be 277.5 nm (compared to 352 nm observed experimentally). Calculations for the ground state did not reveal any minimum for the T form. In the PE curve for the lowest excited singlet state (S_1), there exists a shallow minimum corresponding to the T form, which is much higher in energy than the P. This means that at room temperature one would observe only normal emission. Interestingly, AM1 calculations predict a Stokes shift of 4443 cm^{-1}, when compared to the experimentally observed value of 4485 cm^{-1}. CIS calculations tend to underestimate the Stokes shift (2902 cm^{-1}).

The oscillator strength (f) increases slightly with increase in r_{O_d-H} as shown in Figure 6 for the S_0 to S_1 transition, suggesting that the emission could take place over a range of geometries with λ ranging from 277.5 to 301.8 nm. Both the $S_1(L_b)$ and $S_2(L_a)$ states show $\pi\pi^*$ character. And yet, the oscillator strength for the S_0-S_2 (L_a) transition is significantly lower than that for the S_0-S_1 (L_b) transition, as illustrated in Figure 6, in agreement with the experimental result (see Figure 4i). The oscillator strength for the S_0-S_3 transition, plotted in Figure 6, is found to be about six times larger than that for the S_0-S_1 transition for the P form, in keeping with the observation for the 225 nm band shown in Figure 4i.

Since there is a bond breaking and a bond forming involved in the intramolecular proton transfer, it is expected that the HF

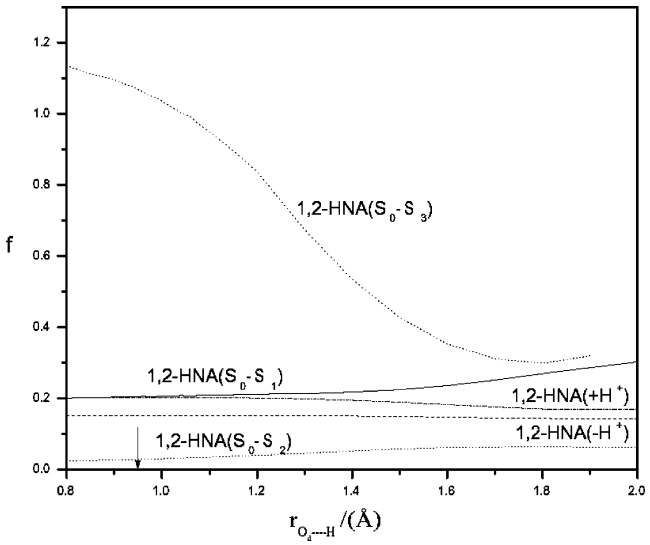

Figure 6. Oscillator strength (f) vs distinguished-coordinate curve for S_0-S_1, S_0-S_2, and S_0-S_3 transitions for 1,2-HNA and for the S_0-S_1 transition for the protonated and deprotonated forms of 1,2-HNA as obtained from CIS/6-31G** calculations. The arrow along the x-axis indicates the equilibrium geometry for the neutral species.

method would not yield reliable PE profiles. Since the CIS method is formally equivalent to the HF for the ground electronic state,[21] it may also be considered inadequate for the purpose.[22] However, it has been shown that the HF and CIS method gives qualitatively correct PE profiles for intramolecular proton transfer in the ground and the first excited electronic state of salicylic acid[2] and that the results were comparable to those from higher order methods such as CASPT2.[20] Qualitatively correct results have been obtained with the CIS method by us for 3,2-HNA[3] and by others for 1-hydroxy-2-acetonaph-

thone.[23] Furthermore, there is hardly any barrier over and above the endothermicity in the PE profiles obtained for 1,2-HNA. Therefore, in the absence of better methods becoming available for large systems such as ours, the CIS method seems to be a reasonable choice at this stage.

3.2.2. Influence of Protonation and Deprotonation. 1,2-HNA becomes protonated with the addition of a mineral acid and deprotonated with the addition of an alkali. To account for the effect of pH on the intramolecular proton transfer in 1,2-HNA, PE curves for the protonated and deprotonated forms of 1,2-HNA have been computed by the CIS/6-31G** method and are included in Figure 5, parts ii and iii, respectively. They reveal only a single well for both the ground and the lowest three excited singlet states of the protonated species [Figure 5ii]. The lack of proton transfer in the protonated form is reinforced by a weak intramolecular hydrogen bond of 1.4 kcal/mol (Table 2). CIS calculations predict qualitatively correctly a decrease in the energy gap between the ground and the first excited electronic state and hence a red shift in λ_{max} on protonation, as shown in Table 3. The separation between the first two excited states increases on protonation, thus accounting for the increase in the separation between L_a and L_b bands in the absorption spectrum and also for the enhancement of optical density for the L_b band.

The deprotonated species involves a strong intramolecular hydrogen bond of 30 kcal/mol. The PE profiles for the deprotonated species plotted in Figure 5iii show that the T form is slightly less stable than the P form in the ground state by $\approx$4 kcal/mol and in the excited state by 3 kcal/mol. The oscillator strength remains essentially constant as the proton is transferred along the reaction coordinate (see Figure 6). The λ_{max} for absorption computed by the CIS/6-31G** method for the deprotonated species is 286.3 nm. For the deprotonated species the energy gap between the ground and the first excited state is slightly less than that for the neutral species, which indicates a slight red shift, in contrast to the experiment, which suggests a slight blue shift (see Table 3). The energy separation between the first two excited states also decreases slightly, thus accounting for the lowering of optical density and a decrease of separation between L_a and L_b bands in the absorption spectrum.

4. Summary and Conclusion

The results presented in this paper are summarized in Scheme 1. At low concentrations, the P form of 1,2-HNA is the only emitting species in nonpolar solvents. The lowest excited state is L_b and it does not undergo ESIPT. With an increase in concentration, there is a red shift in absorption and emission indicating the dimer formation. On adding TEA, 1,2-HNA forms an intermolecular hydrogen bond and it becomes more stabilized in the ground state. On increasing the polarity, the Stokes shift increases along with an increase in nonradiative transition. In polar solvents emission from 1,2-HNA is independent of concentration. It forms protonated and deprotonated species under acidic and basic conditions, respectively. *ESIPT is observed only in the deprotonated form.*

The computed ground state PE profiles reveal a single minimum for the neutral as well as the protonated form of 1,2-HNA, while for the deprotonated species there is a double minimum both in the ground and in the excited state. This accounts for the observed ESIPT in the deprotonated form and a lack of ESIPT in the neutral and protonated forms of 1,2-HNA. The keto form of the deprotonated species is slightly less stable than the enol form in the ground state. The calculated oscillator strength values account qualitatively correctly for the observed relative intensities of the L_a and L_b bands. The shift of the absorption bands (L_a, L_b) due to a change in pH, i.e., on protonation and deprotonation with respect to the neutral species, is also reflected in the computed PE curves.

The spectral properties of 1,2-HNA resemble that of the 3,2-HNA[3] in some respects and differ in some respects. The absorption maximum for the former is nearly 40 nm blue shifted with respect to the latter, presumably due to the cross linking as has been observed in the methylated system.[7] Unlike 3,2 HNA, 1,2-HNA *does not* exhibit ESIPT under neutral conditions. Akin to the anion of 3,2-HNA, the anion of 1,2-HNA also exhibits ESIPT. In addition, the deprotonated form of 1,2-HNA exhibits GSIPT due to the small barrier between the enol and the keto forms. In 1,2-HNA deprotonation takes place for pH $>$12, while in 3,2-HNA it starts taking place at a lower pH. The differences in the photophysical behavior of 1,2-HNA and 3,2-HNA can be attributed to the differences in the hydrogen bonding strength, geometry, and changes in the excited-state pK_a values.

Acknowledgment. One of the authors (H.M.) is thankful to the Council of Scientific and Industrial Research (CSIR), New Delhi for a research associateship. This study was supported in part by a grant from CSIR, New Delhi. We thank Mr. C. N. Ramachandran of IIT Kanpur for carrying out some of the additional CIS calculations.

Note Added after ASAP Publication. Labels in Figure 3 were corrected from the original version published ASAP February 25, 2005. The corrected version was published ASAP March 2, 2005.

References and Notes

(1) Joshi, H. C.; Mishra, H.; Tripathi, H. B. *J. Photochem. Photobiol. A: Chem.* **1997**, *105*, 15.

(2) Maheshwari, S.; Chowdhury, A.; Sathyamurthy, N.; Mishra, H.; Tripathi, H. B.; Panda, M.; Chandrasekhar, J. *J. Phys. Chem. A* **1999**, *103*, 6257.

(3) Mishra, H.; Joshi, H. C.; Tripathi, H. B.; Maheshwary, S.; Sathyamurthy, N.; Panda, M.; Chandrasekhar, J. *J. Photochem. Photobiol. A: Chem.* **2001**, *139*, 23.

(4) Mishra, H.; Misra, V.; Mehata, M. S.; Pant, T. C.; Tripathi, H. B. *J. Phys. Chem. A* **2004**, *108*, 2346.

(5) Schulman, S. G.; Kovi, P. J. *Anal. Chim. Acta* **1973**, *67*, 267.

(6) Tolbert, L. M.; Solntsev, K. M. *Acc. Chem. Res.* **2002**, *35*, 19.

(7) Catalán, J.; del Valle, J. C.; Palomar, J.; Diaz, C.; de Paz, J. L. G. *J. Phys. Chem. A* **1999**, *103*, 10921.

(8) Woolfe, G. J.; Thistlethwaite, P. J. *J. Am. Chem. Soc.* **1981**, *103*, 3849.

(9) Fleming, G. R. *Chemical Applications of Ultrafast Spectroscopy*; Academic: New York, 1986; p 205.

(10) Kovi, P. J.; Shulman, S. G. *Anal. Chem.* **1973**, *45*, 989.

(11) Kovi, P. J.; Miller, C. L.; Schulman, S. G. *Anal. Chim. Acta* **1972**, *61*, 7.

(12) Woolfe, G. J.; Thistlethwaite, P. J. *J. Am. Chem. Soc.* **1980**, *102*, 6917.

(13) Law, K.-Y.; Shoham, J. *J. Phys. Chem.* **1994**, *98*, 3114.

(14) Golubev, N. S.; Denisov, G. S.; Kuzina, L. A.; Smirnov, S. N. *J. General Chem.* (*Russian*) **1994**, *64*, 1162.

(15) Klessinger, M.; Michl, J. *Excited state and photochemistry of organic molecules*; VCH: New York, 1995; p 47.

(16) Banerjee, D.; Mandal, A.; Mukherjee, S. *Chem. Phys. Lett.* **2002**, *357*, 450.

(17) Mishra, H.; Tripathi, H. B.; Pant, D. D. *Rev. Sci. Instrum.* In press.

(18) Joshi, G. C.; Tripathi, H. B.; Pant, D. D. *Ind. J. Phys.* **1986**, *60B*, 7.

(19) Frisch, M. J.; Trucks, G. W.; Schlegel, H. B.; Gill, P. M. W.; Johnson, B. G.; Robb, M. A.; Cheeseman, J. R.; Keith, T.; Petersson, G. A.; Montgomery, J. A.; Raghavachari, K.; Al-Laham, M. A.; Zakrzewski, V. G.; Ortiz, J. V.; Foresman, J. B.; Cioslowski, J.; Stefanov, B. B.; Nanayakkra, A.; Challacombe, M.; Peng, C. Y.; Ayala, P. Y.; Chen, W.; Wong, M. W.; Andres, J. L.; Replogle, E. S.; Gomperts, R.; Martin, R. L.; Fox, D. J.; Binkley, J. S.; Defrees, D. J.; Baker, J.; Stewart, J. P.; Head-

Gordon, M.; Gonzalez, C.; Pople, J. A. *Gaussian 94*, Revision C.2; Gaussian Inc.: Pittsburgh, PA, 1995.

(20) Sobolewski, A. L.; Domcke, W. *Chem. Phys.* **1998**, *232*, 257.

(21) Foresman, J. B.; Head-Gordon, M.; Pople, J. A.; Frisch, M. J. *J. Phys. Chem*. **1992**, *96*, 135.

(22) Catalán, J.; de Paz, J. L. G. *J. Phys. Chem. A* **2001**, *105*, 7315.

(23) Organero, J. A.; Vargas Diaz, A.; Moreno, M.; Santos, L.; Douhal, A. *J. Phys. Chem. A* **2001**, *105*, 7317.

(24) Ab initio investigations of intra and intermolecular proton transfer in salicylic acid and related systems, possibility of proton motion through buckminsterfullerene and related systems and structure and stability of water clusters; Maheshwary, S. Ph.D. Thesis, IIT Kanpur, India, 2000.

(25) Photoinduced electronic excited-state relaxation and proton-transfer phenomena in some hydrogen bonded molecular systems; Mishra, H. Ph.D. Thesis, Kumaun University, India, 2002.